



HAL
open science

Anisotropic Oxygen Diffusion Properties in $\text{Pr}_2\text{NiO}_{4+\delta}$ and $\text{Nd}_2\text{NiO}_{4+\delta}$ Single Crystals

Jean-Marc. Bassat, Monica Burriel, Olivia Wahyudi, Remy Castaining, Monica Ceretti, Philippe Veber, Isabelle Weill, Antoine Villesuzanne, Jean-Claude Grenier, Werner Paulus, et al.

► To cite this version:

Jean-Marc. Bassat, Monica Burriel, Olivia Wahyudi, Remy Castaining, Monica Ceretti, et al.. Anisotropic Oxygen Diffusion Properties in $\text{Pr}_2\text{NiO}_{4+\delta}$ and $\text{Nd}_2\text{NiO}_{4+\delta}$ Single Crystals. *Journal of Physical Chemistry C*, 2013, 117 (50), pp.1932-7447. 10.1021/jp409057k . hal-00920836

HAL Id: hal-00920836

<https://hal.science/hal-00920836>

Submitted on 25 May 2022

HAL is a multi-disciplinary open access archive for the deposit and dissemination of scientific research documents, whether they are published or not. The documents may come from teaching and research institutions in France or abroad, or from public or private research centers.

L'archive ouverte pluridisciplinaire **HAL**, est destinée au dépôt et à la diffusion de documents scientifiques de niveau recherche, publiés ou non, émanant des établissements d'enseignement et de recherche français ou étrangers, des laboratoires publics ou privés.

Anisotropic Oxygen Diffusion Properties in $\text{Pr}_2\text{NiO}_{4+\delta}$ and $\text{Nd}_2\text{NiO}_{4+\delta}$ Single Crystals

Jean-Marc Bassat,^{*,†,‡} Mónica Burriel,^{*,§} Olivia Wahyudi,^{†,‡,⊥} Rémi Castaing,^{†,‡,§} Monica Ceretti,^{||} Philippe Veber,^{†,‡} Isabelle Weill,^{†,‡} Antoine Villesuzanne,^{†,‡} Jean-Claude Grenier,^{†,‡} Werner Paulus,^{||} and John A. Kilner[§]

[†]CNRS, ICMCB, UPR 9048, F-33600 Pessac, France

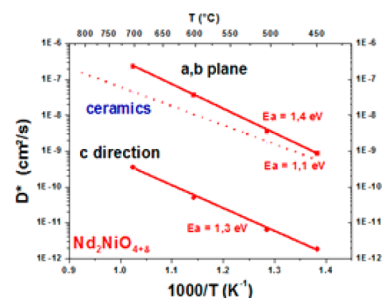
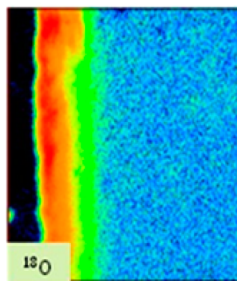
[‡]Univ. Bordeaux, ICMCB, UPR 9048, F-33600 Pessac, France

[§]Department of Materials, Imperial College London, Exhibition Road, London SW7 2AZ, U.K.

^{||}Institut Charles Gerhardt, UMR 5253, Place E. Bataillon, 34095 Montpellier cedex 5, France

[⊥]Université de Rennes 1, UMR 6226, 35042 Rennes cedex, France

ABSTRACT: The anisotropy of the oxygen anionic conductivity was measured for two mixed ionic electronic conducting (MIEC) oxides with the 2D K_2NiF_4 -type structure, i.e., $\text{Nd}_2\text{NiO}_{4+\delta}$ and $\text{Pr}_2\text{NiO}_{4+\delta}$, using high quality single crystals. Measurements of the oxygen diffusivity and surface exchange performed parallel and perpendicularly to the [001] direction, from 450 to 700 °C, using the isotope exchange depth profile (IEDP) technique, combining $^{16}\text{O}/^{18}\text{O}$ exchange and secondary ion mass spectroscopy (SIMS) are reported. For both materials the diffusion is about 3 orders of magnitude higher along the (*a,b*)-plane compared to the perpendicular (*c*-axis) direction. These values are among the highest when compared to several state-of-the-art MIEC materials. The diffusion along the (*a,b*)-plane for $\text{Pr}_2\text{NiO}_{4+\delta}$ is higher than that of $\text{Nd}_2\text{NiO}_{4+\delta}$ due to a much lower diffusion activation energy (0.5 and 1.4 eV for $\text{Pr}_2\text{NiO}_{4+\delta}$ and $\text{Nd}_2\text{NiO}_{4+\delta}$, respectively). A large anisotropy is also observed in the surface exchange coefficient (k^*) values for both materials, with (*a,b*)-plane coefficients being 1 to 1.5 orders of magnitude larger than those for the *c*-axis.



1. INTRODUCTION

The development of new oxide materials for application in high temperature electrochemical energy conversion devices continues to be an area of strong interest. Of the many materials under development, mixed ionic electronic conductors (MIEC) are the materials that show the most fascinating aspects of solid state chemistry due to their high degree of nonstoichiometry. In the past, attention was focused on perovskite structured materials such as $\text{La}_{1-x}\text{Sr}_x\text{CoO}_{3-\delta}$ or $\text{La}_{1-x}\text{Sr}_x\text{Co}_{1-y}\text{Fe}_y\text{O}_{3-\delta}$ that show high degrees of oxygen deficiency.^{1,2} Although these materials display high performances, e.g., as fuel cell cathodes, due to the high mobility of the resulting oxygen vacancies, there has been a recognition that the materials suffer from a number of problems including high chemical expansion coefficients, susceptibility to Cr poisoning, and long-term stability problems due in part to the high degree of oxygen deficiency and aliovalent substitution, particularly by strontium.³

In the past decade this has sparked interest in alternative materials that display nonstoichiometry due to oxygen excess accommodated by oxygen interstitial species such as $\text{La}_2\text{NiO}_{4+\delta}$ and $\text{Pr}_2\text{NiO}_{4+\delta}$ oxides with the K_2NiF_4 -type structure (first member of the so-called Ruddlesden–Popper series).⁴ These structures consist of offset ABO_3 perovskite layers interspersed

by AO rocksalt layers. The oxygen interstitials are thought to have a highly anisotropic mobility migrating by an interstitial mechanism in the rocksalt layers. Oxygen intercalated K_2NiF_4 -type oxides all show large displacements of the apical oxygen atoms (O_{ap}), the interstitial oxygen atoms (O_{int}) being located close to them, i.e., in the (1/4, 1/4, 1/4) site with respect to the $Fmmm$ -type-cell. As a consequence of the resulting short $\text{O}_{\text{int}}-\text{O}_{\text{ap}}$ oxygen distances (about 2.1 Å), the adjacent apical oxygen atoms are shifted away from their average positions in order to form a symmetrically enlarged $\text{O}_{\text{int}}(\text{O}_{\text{ap}})_4$ tetrahedron, thus leading to strong local distortions.⁵ It has been recently shown for $\text{La}_2\text{CuO}_{4.07}$ that these O_{ap} displacements are at least partially of dynamic origin, resulting in an apical oxygen position that is strongly delocalized covering a circle of about 1 Å in diameter and thus strongly favoring displacements toward the interstitial lattice sites.⁶ A similar scenario has been found for $\text{La}_2\text{NiO}_{4+\delta}$.⁷ The dynamic aspect of these displacements becomes important especially at low temperatures, as the related diffusion mechanism has been found to be phonon assisted involving low energy lattice modes, similar to what has been observed for

oxides with brownmillerite-type structure.⁸ For K_2NiF_4 -type oxides the presence of interstitial oxygen atoms seems to be necessary for oxygen diffusion, as it has been modeled for $La_2NiO_{4+\delta}$, thus confirming the necessity of dynamic displacements of the apical oxygen atoms, as experimentally found by high-resolution neutron diffraction. The shallow diffusion potential of the apical oxygen atoms formed by this dynamic disorder scenario should be influenced especially by the c -lattice parameter, as significant variations are observed ranging from 13.15 Å for stoichiometric $La_2CuO_{4.0}$ and 12.52 Å for $La_2NiO_{4.0}$ to only 12.10 Å for $Pr_2NiO_{4.0}$.

In this way the aim of this study is to carefully measure the oxygen diffusion coefficients and associated activation energies for single crystals of both $Pr_2NiO_{4+\delta}$ and $Nd_2NiO_{4+\delta}$ along the two main crystallographic orientations in this highly anisotropic structure, in order to compare these values within this series of compounds.

2. EXPERIMENTAL SECTION

2.1. Crystal Growth. Single crystals of $Pr_2NiO_{4+\delta}$ and $Nd_2NiO_{4+\delta}$ were synthesized using the floating zone (FZ) method by means of an optical mirror furnace (NEC SC3-MDH11020). Specifically, the traveling solvent floating zone (TSFZ) technique in a vertical configuration was used. The apparatus consists of two gold-coated ellipsoidal mirrors that focus the light from halogen lamps onto a vertically held rod-shaped sample; temperatures above 2200 °C were reached, high enough to melt the polycrystalline rods of the nickelates.

First, polycrystalline powders of both materials were prepared by the conventional solid state method. The starting materials used are neodymium oxide, Nd_2O_3 (99.9%, Sigma-Aldrich), praseodymium oxide, Pr_6O_{11} (99.9%, Alfa-Aesar), and nickel oxide, NiO (99%, Alfa-Aesar). Because of the hygroscopic nature of Nd_2O_3 and Pr_6O_{11} , the starting oxide powders were first heated in vacuum at 1173 K overnight to remove any volatile impurities. The NiO powder was also heated at 353 K in an oven overnight. The reactants were then mixed in a stoichiometric ratio and ground in acetone medium. The mixture was first heated at 1523 K for 24 h. After cooling down to room temperature, the mixture was ground and made into pellets (about 1 g each, Φ 10 mm), which were sintered at 1523 K for more than 24 h. The last step was repeated two times, which leads to a total of about 72 h of sintering. The purity of the $Ln_2NiO_{4+\delta}$ powder samples was verified by conventional X-ray diffraction (XRD). Finally, seed and feed rods were prepared by pressing the powders under hydrostatic pressure (about 10 MPa) and then sintering again. The rods have to be uniform in length, diameter, and density.

The first step of crystal growth is to melt the starting material and then to connect, via the liquid phase called the molten zone, the seed and feed rods. The molten zone is thus located in between the two rods that rotate (about 30 rpm) in opposite direction, and it is then moved (about 2–3 mm/h) along the feed rod through the focus in order to crystallize the liquid phase on the seed. The stability of the molten zone is controlled by visual observation and manual adjustments, with a CDD camera. Since the crystallization was found to be more difficult specifically for $Pr_2NiO_{4+\delta}$, a seed crystal was used for the growth, instead of a polycrystalline sample, as was the case for $Nd_2NiO_{4+\delta}$. In contrast to what has been observed for $La_2NiO_{4+\delta}$,⁹ the partial volatility of nickel creates instability during crystal growth. Therefore, the polycrystalline powders used to make the rods were synthesized adding excess of NiO;

repeated attempts led to determine the optimum excess to be 2%.

Single crystals for both compositions were successfully grown under an O_2 atmosphere. Their length was usually about 80–95 mm with diameter of 6.5 mm, as shown in Figure 1.

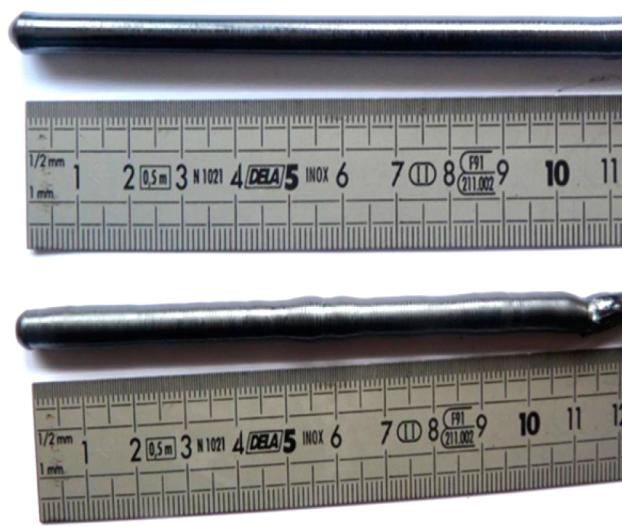


Figure 1. Single crystals of $Nd_2NiO_{4+\delta}$ (top) and $Pr_2NiO_{4+\delta}$ (bottom) grown by the floating zone method.

X-ray diffraction data were taken on a small section of both crystals that was crushed into fine powders. It was found that the crystals consist of a mixture of two phases with similar lattice parameters, both belonging to the $Fmmm$ space group. After heat treatment at about 700 K for four days, all samples were found to be single phase (space group $Fmmm$), as illustrated for $Nd_2NiO_{4+\delta}$ in Figure 2.

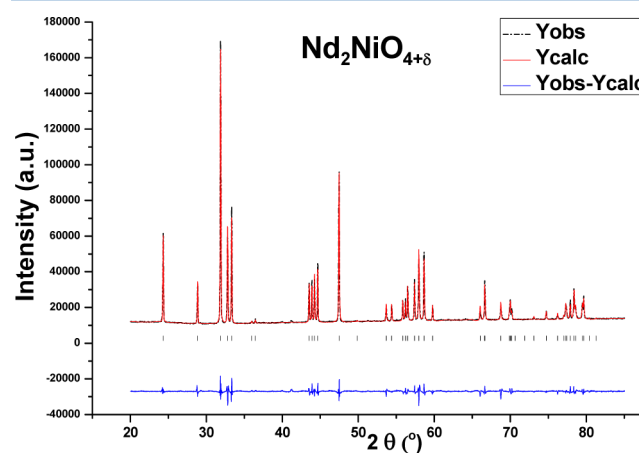


Figure 2. XRD of a crushed $Nd_2NiO_{4+\delta}$ ($\delta = 0.22$) single crystal after heat treatment at 700 K.

The chemical composition and homogeneity of the crystals were checked by using EDS analysis and SEM observations. The cationic ratio Nd (or Pr) over Ni measured at each point of the analyzed cross-section was close to 2. The crystallinity of the single crystals was checked by Laue X-ray diffraction. The oxygen content was determined by two ways, i.e., (i) thermogravimetric analysis (TGA) carried out under a reducing atmosphere (flowing 5% H_2 in Ar); for this purpose about 100

mg of powder was heated up to 900 °C with heating rate of 1 °C/min, and (ii) iodometric titration of powder obtained by crushing a piece of the single crystal. Both methods give the amount of present Ni³⁺ and thereby, by deduction, the oxygen content of the sample at room temperature. Using both methods, the oxygen excesses were estimated to be $\delta = 0.20$ and $\delta = 0.22$ for Nd₂NiO_{4+ δ} and Pr₂NiO_{4+ δ} , respectively. These high δ values, together with a mixed Ni²⁺/Ni³⁺ valence for nickel, lead to the well-known MIEC properties for both materials. For both materials, oxygen will be progressively lost as the temperature is raised. Nevertheless relatively high oxygen nonstoichiometry values are maintained at high temperatures (e.g., $\delta = 0.12$ for Pr₂NiO_{4+ δ} and $\delta = 0.15$ for Nd₂NiO_{4+ δ} at 700 °C), as reported by Boehm et al.¹⁰ Thus, it is expected that the mixed conducting properties will be maintained at the electrode operating temperatures ($T > 500$ °C).

2.2. Crystal Orientation. Because of the very high expected anisotropy ratio of the oxygen diffusion in these nickelates with regard to previous results,^{11,12} it has been shown that it is essential to have a misalignment angle, Θ , of the crystallographic faces lower than 1.5° in order to perform accurate measurements, especially for the short diffusion lengths along the c -axis.¹³

In this way, single crystals fixed on a HUBER 1006 goniometer head were orientated along the main crystallographic axes using the Laue back scattering method. A S203.10 HUBER 2-circle segment rotation device was used to correct the crystal misalignment during the orientation process. The diffraction patterns were collected either on KODAK photographic films or with a CCD-camera device using polychromatic X-rays Bremsstrahlung (white beam) supplied by a copper anticathode (40 mA; 40 kV). Experimental patterns were then indexed with the Orient-express software allowing us to orientate crystals with an accuracy of 0.01°.

The cutting of the crystals was performed with a diamond wire saw ESCIL equipped with a 2 circle Microcheck orientation system on which the goniometer head can be positioned.

Finally, after a slight polishing of the edges, the orientation of the cut faces was checked by the Laue diffraction method using a silicon single crystal as a reference. The misalignment between the (511) crystal face and its mechanical plane was considered to be less than 0.01° for the reference single crystal. This allowed to reproduce the positioning of the crystal cut faces parallel to the (511) silicon face and perpendicular to the X-rays beam with an absolute accuracy being in each case, thanks to our updated equipment, less than 1° along the 2-circle-segment axis, which satisfies the initial requirement for performing the diffusion measurements.

2.3. Oxygen Isotopic Exchange and Secondary Ion Mass Spectrometry Measurements. The oxygen diffusion and surface exchange phenomena, characterized by the D^* and k^* coefficients, was determined by measuring the diffusion of an oxygen isotope (¹⁸O) using the so-called isotope exchange depth profile (IEDP) technique.¹⁴ The secondary ion mass spectrometry (SIMS) analyses were carried out in two different laboratories: Institut de Chimie de la Matière Condensée de Bordeaux (ICMCB) and Imperial College London (IC), while the oxygen exchanges were performed at ICMCB only. Prior to the oxygen exchange, polished crystal samples were first thermodynamically equilibrated in a quartz tube, under a partial pressure (0.21 atm) of natural oxygen (¹⁶O, 99.75%) by annealing at given temperatures corresponding to the exchange

temperatures, during several hours. To ensure that the material had reached thermodynamic equilibrium at the operating temperature and pressure, the duration of this anneal step was about 12 h, which is much longer than the isotope exchange length of time. At the end of the equilibration stage, the sample was quenched down to room temperature. The atmosphere in the tube was then replaced by ¹⁸O (97% from Euriso-top), and the samples were exchanged at the same temperature and same partial pressure (0.21 atm) for a given time. This exchange time was estimated on the basis of previous measurements carried out on La₂NiO_{4+ δ} single crystals and depends on the crystallographic direction and temperature.¹² Isotopic exchange experiments were performed at several temperatures in the range 450–700 °C.

After the isotope exchange, the samples were first cut perpendicular to the exchanged surface, parallel to the direction of interest, and the cross-section was polished prior to the measurement. The samples were then embedded in Woods alloy (Goodfellow) and polished using abrasive paper of decreasing roughness (until 0.25 μ m). The ¹⁸O and ¹⁶O concentration depth profiles were measured by SIMS. The SIMS analyses performed at ICMCB were done using a Cameca IMS 6F device with Cs⁺ ions as incident ions. Two different modes of analysis were used: the linescan mode, when the penetration depth profiles are higher than 250 μ m, and the surface scanning mode, when profiles are less than 250 μ m. When surface scanning mode was used, an image over a zone of 50 × 50 μ m² was digitized to obtain accurate profile determinations. All the exchanged samples studied at IC were measured on a ToF-SIMS 5 instrument (ION-TOF GmbH, Münster, Germany) equipped with bismuth pulsed liquid metal ion gun (25 keV) incident at 45° (analysis beam), using the burst alignment mode (7 or 8 peaks). The imaging mode, described in detail by De Souza et al.,¹⁴ was used for the measurement of the oxygen diffusion. This mode was selected as it permits the visualization of the distribution of the species in the analyzed area using a high lateral resolution. In both cases, the main experimental difficulty being to determine the perpendicular diffusion (along the c -axis) *without overestimating it*, it was of high importance to accurately orientate the crystals as previously stressed.

3. RESULTS

Since the sample thickness is sufficiently large in comparison to the ¹⁸O tracer penetration depth, the measured penetration profile can be fitted using a solution for Fick's second law proposed by Crank,¹⁵ applied for diffusion into a semi-infinite medium. It is assumed that the source concentration is constant with respect to time and that the oxygen flux is limited by the surface exchange reactions. Mathematically, the normalized concentration $C(x)$ of ¹⁸O is

$$C(x) = \operatorname{erfc}\left(\frac{x}{2\sqrt{D^*t}}\right) - \exp\left(\frac{k}{D^*}x + \frac{k^2}{D^*}t\right) \operatorname{erfc}\left\{\left(\frac{x}{2\sqrt{D^*t}}\right) + \left(\frac{k}{D^*}\sqrt{D^*t}\right)\right\}$$

where x is the profile depth, D^* is the tracer oxygen diffusion coefficient, k^* is the tracer surface exchange coefficient, and t is the exchange duration.

Figure 3 shows, as an example, the color gradation in the concentration of ¹⁶O and ¹⁸O obtained by the surface scanning

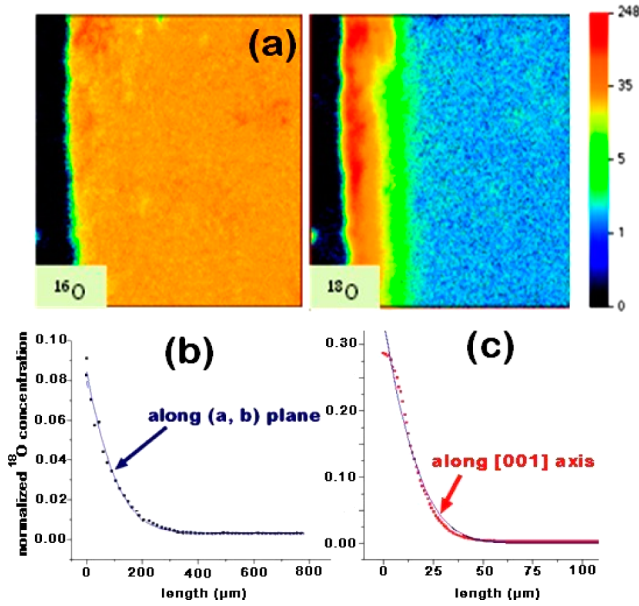


Figure 3. (a) ^{16}O and ^{18}O SIMS images (along the c -axis) showing the color gradation in the concentrations obtained by the surface scanning method, (b) normalized ^{18}O concentration profile extract along the (a,b) -plane direction (recorded using the line-scanning method), and (c) normalized ^{18}O concentration profile extract along the c -axis (obtained from previous images). Both profiles correspond to the $\text{Nd}_2\text{NiO}_{4+\delta}$ crystal exchanged at 703 °C during 856 s.

method (here performed along the c -axis) on a $\text{Nd}_2\text{NiO}_{4+\delta}$ crystal exchanged at 703 °C during 856 s. Normalized ^{18}O concentration profiles recorded along the two main crystallographic directions, on the same crystal using the same exchange conditions, are also compared in Figure 3.

Figure 4 summarizes the measured D^*_{ab} and D^*_c values for $\text{Nd}_2\text{NiO}_{4+\delta}$ as a function of temperature. For the whole

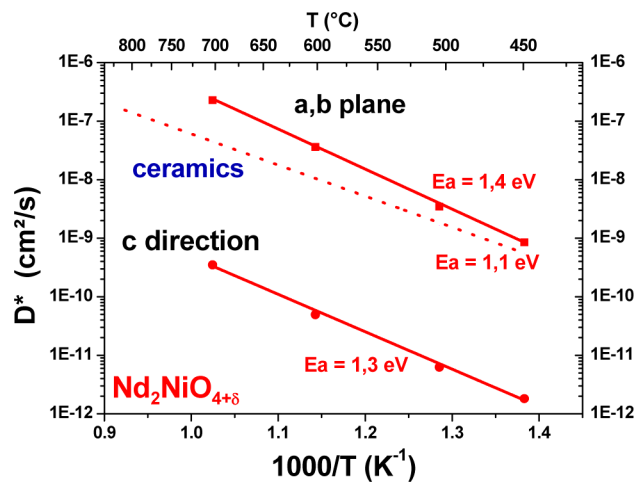


Figure 4. D^* vs $1000/T$ for $\text{Nd}_2\text{NiO}_{4+\delta}$ single crystal (solid lines) and comparison with polycrystalline ceramics from ref 10 (dotted line).

measured temperature range, the oxygen diffusion in the (a,b) -plane of the single crystal is about 3 orders of magnitude higher than the corresponding value along the c -axis. The value of the diffusion coefficient for ceramic samples is close to the (a,b) -plane one.¹⁰ This suggests that (a,b) -plane diffusion process dominates for polycrystalline materials. The activation energy

of the oxygen diffusion does not depend on the crystallographic orientation, being about $E_a = 1.4 (\pm 0.2)$ and $1.3 (\pm 0.2)$ eV for the (a,b) -plane and c -axis, respectively, which are unexpectedly high values, particularly for the (a,b) -plane. Finally, the diffusion in the (a,b) -plane, for example, at $T = 600$ °C, appears to be larger than the ones measured for most of the current MIEC materials studied as SOFC cathodes.¹⁶

The diffusion in the (a,b) -plane is larger for $\text{Pr}_2\text{NiO}_{4+\delta}$ compared to $\text{Nd}_2\text{NiO}_{4+\delta}$ (Figure 5) and $\text{La}_2\text{NiO}_{4+\delta}$ ^{11,12}

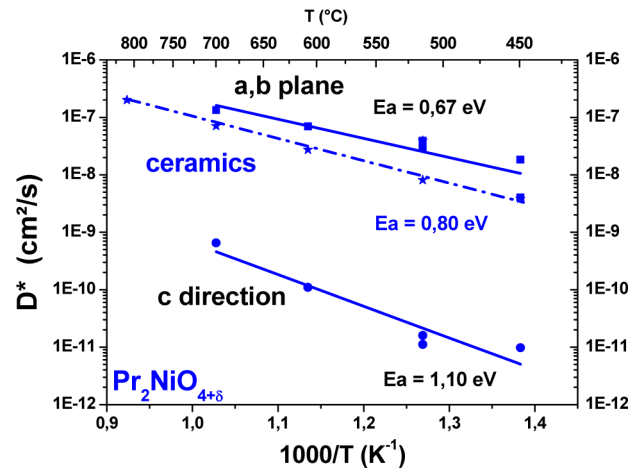


Figure 5. D^* vs $1000/T$ for $\text{Pr}_2\text{NiO}_{4+\delta}$ single crystal (solid lines) and comparison with polycrystalline ceramics from ref 10 (dotted line).

especially in the low temperature range. This is due to the small activation energy of the diffusion in $\text{Pr}_2\text{NiO}_{4+\delta}$, which is about one-half the one for the neodymium compound ($0.67 (\pm 0.1)$ eV and $1.4 (\pm 0.2)$ eV, respectively). Both sets of data (measurements performed at ICMCB and IC) give results that are in good agreement. Once again the value of the diffusivity for the ceramic $D^*(\text{ceramic})$ is close to the diffusivity along the (a,b) -plane (D^*_{ab}) for all temperatures, while the activation energy of the oxygen diffusion in the ceramics is intermediate between the values measured for the two main crystallographic orientations of the single crystal.

4. DISCUSSION

In this kind of oxygen overstoichiometric oxides, it seems to be well established that the key point for the oxygen mobility is the intrinsic disorder occurring between both the apical and interstitial sites.¹⁷ Indeed the diffusion mechanism along the (a,b) -plane is not, as might be first expected, a direct displacement of the oxygen ions along interstitial site paths but is rather a so-called interstitialcy (or push-pull) mechanism in which the labile apical oxygen is also involved: first, the apical oxygen moves into the interstitial site in the rock-salt-type layer; then, in a second step, the resulting oxygen vacancy at apical site is filled by a nearby interstitial oxygen. This mechanism was suggested by atomistic studies on $\text{La}_2\text{NiO}_{4+\delta}$ ¹⁸ and has been evidenced latter by neutron diffraction on $(\text{Pr}_{0.9}\text{La}_{0.1})_2(\text{Ni}_{0.74}\text{Cu}_{0.21}\text{Ga}_{0.05})\text{O}_{4+\delta}$ at high temperatures.¹⁹

According to molecular dynamics (MD) calculations,^{17,20} the corresponding activation energy would range between 0.5 and 0.7 eV, in good agreement with our measurements for $\text{La}_2\text{NiO}_{4+\delta}$.¹² For $\text{Pr}_2\text{NiO}_{4+\delta}$, MD simulations concluded that the activation energy of the oxygen diffusion varies between 0.49 and 0.64 eV, depending on the content of oxygen

overstoichiometry.²¹ Such values are also in good agreement with our measurements (Figure 5).

On the contrary, the value of $E_a(a,b)$ measured for $\text{Nd}_2\text{NiO}_{4+\delta}$ is surprisingly high, especially regarding the oxygen diffusion values themselves that are very close to those measured for Pr and La at the highest temperatures ($T \geq 600$ °C). Indeed, the oxygen diffusion coefficients at $T = 700$ °C are quite similar in both materials ($D^* \approx 1-2 \cdot 10^{-7} \text{ cm}^2 \cdot \text{s}^{-1}$), while they differ by 1 order of magnitude at $T = 500$ °C ($D^* \approx 3 \cdot 10^{-8} \text{ cm}^2 \cdot \text{s}^{-1}$ for $\text{Pr}_2\text{NiO}_{4+\delta}$ vs $D^* \approx 3 \cdot 10^{-9} \text{ cm}^2 \cdot \text{s}^{-1}$ for $\text{Nd}_2\text{NiO}_{4+\delta}$). This means that the oxygen mobility is less favored at low temperatures in $\text{Nd}_2\text{NiO}_{4+\delta}$. As a difference between both materials, the possible mixed valence state between 3+ and 4+ only for Pr cation could be considered. However, to the best of our knowledge, Pr^{4+} has never been experimentally observed in $\text{Pr}_2\text{NiO}_{4+\delta}$. Our recent measurements performed by XANES confirmed that only Pr^{3+} can be evidenced. This is in agreement with general steric considerations: because of its too small cationic size, Pr^{4+} cannot be stabilized in this K_2NiF_4 structure. However, an explanation can be attempted considering the results obtained by Bhavaraju et al.:²² using electrochemical intercalation experiments, the authors evidenced that stoichiometric $\text{Nd}_2\text{NiO}_{4.00}$ is obtained by the initial electrochemical reduction of the starting material $\text{Nd}_2\text{NiO}_{4.18}$, but further reoxidation leads to a composition of only $\text{Nd}_2\text{NiO}_{4.10}$ (oxygen overstoichiometric). On the contrary, $\text{La}_2\text{NiO}_{4+\delta}$ exhibits a full reversibility over a range extending up to 0.26.^{23,24} Full reversibility has also been reported for $\text{La}_2\text{CuO}_{4+\delta}$ in the total range of $\delta_{\text{max}} = 0.07$.²⁵ Such a difference in behavior between both materials is assigned to the effect of structural differences. Comparing the structures of $\text{Nd}_2\text{NiO}_{4+\delta}$ to those of $\text{La}_2\text{CuO}_{4+\delta}$ and $\text{La}_2\text{NiO}_{4+\delta}$ indicates that there might be a critical value for the c lattice parameter, below which oxygen intercalation is no longer reversible. From the refined structure, it is clearly seen that the short c parameter results in both a short interoctahedral space (compared to the corresponding La-nickelates) and in a significantly distorted tetrahedral site for interstitial oxygen. Both effects could lead to the hindering of the oxygen diffusion at low temperatures.

Furthermore, it is assumed that an interplay between lattice dynamics and structural instabilities in K_2NiF_4 -type structures exists, which is intimately related to the different oxygen intercalation behaviors of $\text{Nd}_2\text{NiO}_{4+\delta}$, compared to $\text{La}_2\text{NiO}_{4+\delta}$ and $\text{La}_2\text{CuO}_{4+\delta}$. Reduced apical oxygen mobility at moderate temperature would be due to the absence of low energy specific phonon modes. As already seen for $\text{La}_2\text{CuO}_{4+\delta}$,⁶ low energy phonon modes become a general prerequisite for oxygen mobility at moderate (i.e., room) temperature, when thermal vibrations are less significant. Accordingly, some of us demonstrated both experimentally and theoretically that the oxygen mobility occurring at moderate temperature in brownmillerite-type structures (such as $\text{SrCoO}_{2.5}$ and $\text{SrFeO}_{2.5}$) is related unambiguously to low energy phonon modes.⁸ Although brownmillerite- and K_2NiF_4 -type structures are different and have low energy phonons of different nature, as shown by previous calculations,^{6,8} it is believed that such modes play a significant role for oxygen mobility in $\text{Pr}_2\text{NiO}_{4+\delta}$; however, their effect might be less pronounced in the case of $\text{Nd}_2\text{NiO}_{4+\delta}$ related to the slightly smaller c -axis parameter compared to the Pr homologue. This assumption has to be checked by performing electronic structure and lattice dynamics calculations, in situ electrochemical oxygen intercalation coupled with neutron diffraction measurements, as well

as careful inelastic neutron diffusion experiments on single crystals. Such differences in terms of interlayer distances, lattice dynamics, and oxygen disorder, as well as the inter-relation between these three factors, could explain the lower oxygen mobility along the (a,b) -plane in $\text{Nd}_2\text{NiO}_{4+\delta}$ at low temperatures.

On the contrary, the oxygen diffusion coefficients of $\text{Pr}_2\text{NiO}_{4+\delta}$ and $\text{Nd}_2\text{NiO}_{4+\delta}$ measured along the c -axis have very similar values over the whole temperature range, with exactly the same activation energy. The migration along the c -axis, occurring via a direct vacancy mechanism, requires significantly higher activation energy. Thus, to give a better insight of the exact diffusion mechanism and pathways along the c -axis, lattice dynamics studies are needed, for instance, by in situ measurements during redox reactions in $\text{Pr}_2\text{NiO}_{4+\delta}$ and $\text{Nd}_2\text{NiO}_{4+\delta}$ single crystals. Moreover, the delocalization of the apical oxygen preferentially in the (a,b) -plane of the structure should be evidenced from neutron single crystal diffraction data using a maximum entropy analysis. This work is in progress.

The thermal evolution of the surface exchange coefficients k^* is shown in Figure 6 for both materials. A large anisotropy is

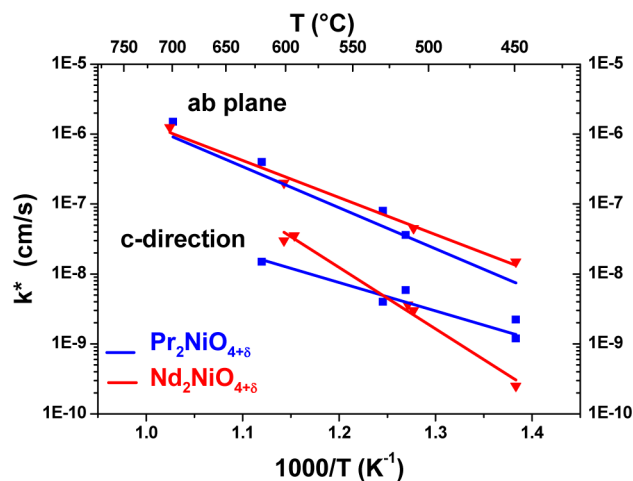


Figure 6. k^* vs $1000/T$ for $\text{Nd}_2\text{NiO}_{4+\delta}$ and $\text{Pr}_2\text{NiO}_{4+\delta}$ single crystals.

observed for both materials over the whole temperature range, with (a,b) -plane coefficients being 1 to 1.5 orders of magnitude larger than the c -axis values. When compared with the data obtained for ceramic samples,¹⁰ the polycrystalline surface exchange coefficients are closer to the k^* values for the (a,b) -plane, which would mean that the crystallographic orientations with the highest surface exchange coefficient are the ones that dominate the process in polycrystalline materials. The activation energies of the surface exchange are high in both directions (>1.3 eV, except along the c -direction for $\text{Pr}_2\text{NiO}_{4+\delta}$ in which it is quite low, 0.8 eV), without clear trends as a function of the rare-earth or the crystallographic direction.

Finally, $\text{Pr}_2\text{NiO}_{4+\delta}$ presents the highest values of both k^* and D^* , which leads to a material with very good electrochemical performances that can be used as an oxygen electrode either in a SOFC device operating at 600 °C,²⁶ or in a high temperature steam electrolysis (HTSE) one at 700–800 °C,²⁷ as has been previously reported in the literature.

5. CONCLUSIONS

$\text{Ln}_2\text{NiO}_{4+\delta}$ (Ln = La, Pr, Nd) rare-earth nickelates are considered as promising oxygen electrode materials. Among

them, $\text{Nd}_2\text{NiO}_{4+\delta}$ and especially $\text{Pr}_2\text{NiO}_{4+\delta}$ exhibit the most interesting electrochemical properties. Knowledge of the relevant oxygen transport parameters (i.e., oxygen transport coefficients D^* and surface exchange constants k^*) in such oxides with MIEC properties is of high importance, especially for understanding the oxygen transport mechanisms in these materials with highly anisotropic properties.

By experimentally tracing the isotopic oxygen ion concentration as a function of depth using the IEDP/SIMS technique, it was possible to determine for the first time the oxygen transport coefficients D^* and surface exchange constants k^* , along the two main crystallographic directions (the (a,b) -plane and the c -axis direction) for both materials. Reliable data were obtained due to the very high quality of the single crystals and to the crystallographic orientations, which were beforehand performed with an accuracy of less than 1° along the two considered directions. Over the whole temperature range (450–700 °C) the oxygen diffusion along the (a,b) -plane is about 3 orders of magnitude larger than along the c -axis, for both materials. The value of the diffusion coefficient for ceramic samples is close to the value measured for the (a,b) -plane, suggesting that (a,b) -plane diffusion process dominates for ceramic materials. As a general trend, the diffusion along the (a,b) -plane is larger compared to most of the state-of-the-art MIEC materials studied as SOFC cathodes.

Some differences were found between both materials when comparing the oxygen diffusion coefficients D^* . The diffusion along the (a,b) -plane is larger for $\text{Pr}_2\text{NiO}_{4+\delta}$ compared to $\text{Nd}_2\text{NiO}_{4+\delta}$. Moreover, the activation energy of the diffusion in $\text{Pr}_2\text{NiO}_{4+\delta}$ is about half the value for the neodymium, which is surprisingly high (~ 0.7 and 1.4 eV, respectively). On the contrary, the oxygen diffusion coefficients of $\text{Nd}_2\text{NiO}_{4+\delta}$ and $\text{Pr}_2\text{NiO}_{4+\delta}$ measured along the c -axis have very similar values for the whole temperature range, with similar activation energy ($E_a \approx 1.1$ – 1.3 eV) for the oxygen diffusion process.

A large anisotropy is also observed for the k^* values for both materials, with (a,b) -plane coefficients 1 to 1.5 orders of magnitude larger than c -axis coefficients. Once again the polycrystalline surface exchange coefficients are closer to the k^* values for the (a,b) -plane, indicating that the oxygen exchange process is dominating in this direction.

Finally, the material having the highest k^* and D^* values, i.e., $\text{Pr}_2\text{NiO}_{4+\delta}$ exhibits very good electrochemical performances as oxygen electrode in SOFC or HTSE devices.

In order to get a better insight in the diffusion mechanism, we are now investigating structural studies of $\text{Pr}_2\text{NiO}_{4+\delta}$ and $\text{Nd}_2\text{NiO}_{4+\delta}$ on single crystals by neutron diffraction, with the aim to directly access the delocalization of the apical oxygen atoms for comparison with previous studies on $\text{La}_2\text{CuO}_{4.07}$.

AUTHOR INFORMATION

Corresponding Authors

*(J.-M.B.) Tel: +33-540-00-27-53. Fax: +33-540-00-27-61. E-mail: bassat@icmcb-bordeaux.cnrs.fr.

*(M.B.) E-mail: monicaburriel@gmail.com.

Notes

The authors declare no competing financial interest.

ACKNOWLEDGMENTS

This research was partly supported by a Marie Curie Intra European Fellowship within the seventh European Community Framework Program (PIEF-GA-2009-252711) (for M.B.). J-

M.B., O.W., M.C., I.W., A.V., and W.P. are grateful for financial support obtained through the ANR project FUSTOM (ANR-08-BLAN-0069).

REFERENCES

- (1) Sun, C.; Hui, R.; Roller, J. Cathode Materials for Solid Oxide Fuel Cells: a Review. *J. Solid State Electrochem.* **2010**, *14*, 1125–1144.
- (2) Mai, A.; Haanappel, V. A. C.; Uhlenbruck, S.; Tietz, F.; Stöver, D. Ferrite-Based Perovskites as Cathode Materials for Anode-Supported Solid Oxide Fuel Cells: Part I. Variation of Composition. *Solid State Ionics* **2005**, *176*, 1341–1350.
- (3) Tucker, M. C.; Kurokawa, H.; Jacobson, C. P.; De Jonghe, L. C.; Visco, S. J. A Fundamental Study of Chromium Deposition on Solid Oxide Fuel Cell Cathode Materials. *J. Power Sources* **2006**, *160*, 130–136.
- (4) Taracón, A.; Burriel, M.; Santiso, J.; Skinner, S. J.; Kilner, J. A. Advances in Layered Oxide Cathodes for Intermediate Temperature Solid Oxide Fuel Cells. *J. Mater. Chem.* **2010**, *20*, 3799–3813.
- (5) Jorgensen, J. D.; Dabrowski, B.; Pei, S.; Richards, D. R.; Hinks, D. G. Structure of the Interstitial Oxygen Defect in $\text{La}_2\text{NiO}_{4+\delta}$. *Phys. Rev. B* **1989**, *40*, 2187–2199.
- (6) Villesuzanne, A.; Paulus, W.; Cousson, A.; Hosoya, S.; Le Dréau, L.; Hernandez, O.; Prestipino, C.; Houchati, M. I.; Schefer, J. On the Role of Lattice Dynamics on Low Temperature Oxygen Mobility in Solid Oxides: a Neutron Diffraction and First-Principles Investigation of $\text{La}_2\text{CuO}_{4+\delta}$. *J. Solid State Electrochem.* **2011**, *15*, 357–366.
- (7) Paulus, W.; Cousson, A.; Dhalenne, G.; Berthon, J.; Revcolevski, A.; Hosoya, S.; Treutmann, W.; Heger, G.; Le Toquin, R. Neutron Diffraction Studies of Stoichiometric and Oxygen Intercalated La_2NiO_4 Single Crystals. *Solid State Sci.* **2002**, *4*, 565–573.
- (8) Paulus, W.; Schober, H.; Eibl, S.; Johnson, M.; Berthier, T.; Hernandez, O.; Ceretti, M.; Plazanet, M.; Conder, K.; Lamberti, C. Lattice Dynamics to Trigger Low Temperature Oxygen Mobility in Solid Oxide Ion Conductors. *J. Am. Ceram. Soc.* **2008**, *130*, 16080–16085.
- (9) Dembinski, K.; Bassat, J. M.; Coutures, J. P.; Odier, P. Crystal Growth of La_2NiO_4 by the Floating Zone Method with a CW CO_2 Laser: Preliminary Characterizations. *J. Mater. Sci. Lett.* **1987**, *6*, 1365–1367.
- (10) Boehm, E.; Bassat, J. M.; Dordor, P.; Mauvy, F.; Grenier, J. C.; Stevens, P. Oxygen Diffusion and Transport Properties in Non-Stoichiometric $\text{Ln}_2\text{NiO}_{4+\delta}$ Oxides. *Solid State Ionics* **2005**, *176*, 2717–2725.
- (11) Burriel, M.; Garcia, G.; Santiso, J.; Kilner, J. A.; Chater, R.; Skinner, S. J. Anisotropic Oxygen Diffusion Properties in Epitaxial Thin Films of $\text{La}_2\text{NiO}_{4+\delta}$. *J. Mater. Chem.* **2008**, *18*, 416–422.
- (12) Bassat, J. M.; Odier, P.; Villesuzanne, A.; Marin, C.; Pouchard, M. Anisotropic Ionic Transport Properties in $\text{La}_2\text{NiO}_{4+\delta}$ Single Crystals. *Solid State Ionics* **2004**, *167*, 341–347.
- (13) Gauquelin N. *Impact of the Structural Anisotropy of $\text{La}_2\text{NiO}_{4+\delta}$ on High Temperature Surface Modifications and Diffusion of Oxygen*. Ph.D. thesis, Aachen, Germany, 2010.
- (14) De Souza, R.; Zehnpfenning, J.; Martin, M.; Maier, J. Determining Oxygen Isotope Profiles in Oxides with Time-of-Flight SIMS. *Solid State Ionics* **2005**, *176*, 1465–1471.
- (15) Crank, J. *The Mathematics of Diffusion*, 2nd ed.; Clarendon Press, Oxford, U.K., 1975.
- (16) Chronos, A.; Yildiz, B.; Tarancon, A.; Parfitt, D.; Kilner, J. A. Oxygen Diffusion in Solid Oxide Fuel Cell Cathode and Electrolyte Materials: Mechanistic Insights from Atomistic Simulations. *Energy Environ. Sci.* **2011**, *4*, 2774–2789.
- (17) Chronos, A.; Parfitt, D.; Kilner, J. A.; Grimes, R. W. Anisotropic Oxygen Diffusion in Tetragonal $\text{La}_2\text{NiO}_{4+\delta}$: Molecular Dynamics Calculations. *J. Mater. Chem.* **2010**, *20*, 266–270.
- (18) Minervini, L.; Grimes, R. W.; Kilner, J. A.; Sickafus, K. E. Oxygen Migration in $\text{La}_2\text{NiO}_{4+\delta}$. *J. Mater. Chem.* **2000**, *10*, 2349–2354.

- (19) Yashima, M.; Enoki, E.; Wakita, T.; Ali, A. R.; Matsushita, Y.; Izumi, F.; Ishihara, T. Structural Disorder and Diffusional Pathway of Oxide Ions in a Doped Pr_2NiO_4 -based Mixed Conductor. *J. Am. Ceram. Soc.* **2008**, *130*, 2762–2763.
- (20) Chroneos, A.; Vovk, R. V.; Goulatis, I. L.; Goulatis, L. I. Oxygen Transport in Perovskite and Related Oxides: A Brief Review. *J. Alloys Compd.* **2010**, *494*, 190–195.
- (21) Parfitt, D.; Chroneos, A.; Kilner, J. A.; Grimes, R. W. Molecular Dynamics Study of Oxygen Diffusion in $\text{Pr}_2\text{NiO}_{4+\delta}$. *Phys. Chem. Chem. Phys.* **2010**, *12*, 6834–6836.
- (22) Bhavaraju, S.; Di Carlo, J. F.; Scarfe, D. P.; Yazdi, I.; Jacobson, A. J. Electrochemical Intercalation of Oxygen in $\text{La}_2\text{NiO}_{4+x}$ ($0 \leq x \leq 0.18$) at 298 K. *Chem. Mater.* **1994**, *6*, 2172–2176.
- (23) Grenier, J. C.; Wattiaux, A.; Demourgues, A.; Pouchard, M.; Hagenmuller, P. Electrochemical Oxidation: a New Way for Preparing High Oxidation States of Transition Metals. *Solid State Ionics* **1993**, *63*, 825–832.
- (24) Grenier, J. C.; Pouchard, M.; Wattiaux, A. Electrochemical Synthesis: Oxygen Intercalation. In *Current Opinion in Solid State and Materials Science*; Rouxel, J., Rao, C. N. R., Eds.; Elsevier: New York, 1996; Vol. 1, pp 233–240.
- (25) Paulus, W.; Heger, G.; Rudolf, P.; Schöllhorn, R. In Situ Neutron Diffraction Studies on the Electrochemical Oxidation of Polycrystalline La_2CuO_4 . *Phys. C* **1994**, *235–240*, 861–862.
- (26) Ferchaud, C.; Grenier, J. C.; Zhang-Steenwinkel, Y.; van Tuel, M. M. A.; van Berkel, F. P. F.; Bassat, J. M. High Performance Praseodymium Nickelate Oxide Cathode for Low Temperature Solid Oxide Fuel Cell. *J. Power Sources* **2011**, *196*, 1872–1879.
- (27) Ogier, T.; Bassat, J. M.; Mauvy, F.; Fourcade, S.; Grenier, J. C.; Couturier, K.; Petitjean, M.; Mougín, J. Enhanced Performances of Structured Oxygen Electrodes for High Temperature Steam Electrolysis. *Fuel Cells* **2013**, *13*, 536–541.